

Structure and Magnetic Properties of KRuO₄

Casey A. Marjerrison,[†] Cole Mauws,[‡] Arzoo Z. Sharma,[‡] Christopher R. Wiebe,^{‡,#} Shahab Derakhshan,[§] Chad Boyer,^{||} Bruce D. Gaulin,^{†,‡,§} and John E. Greedan*,^{†,‡,§}

[†]Department of Physics and Astronomy and [‡]Brockhouse Institute for Materials Research, McMaster University, Hamilton, Ontario L8S 4M1, Canada

[‡]Department of Chemistry, University of Winnipeg, Winnipeg, Manitoba R3B 2E9, Canada

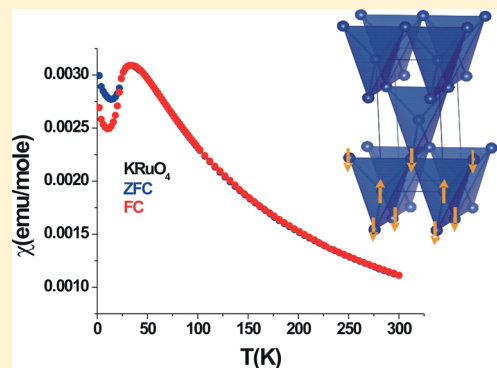
[§]Department of Chemistry and Biochemistry, California State University at Long Beach, Long Beach, California 90840-9507, United States

^{||}Canadian Neutron Beam Centre, Canadian Nuclear Laboratories, Chalk River, Ontario K0J 1J0, Canada

*Canadian Institute for Advanced Research, Toronto, Ontario M5G 1Z8, Canada

Supporting Information

ABSTRACT: The crystal structure of KRuO₄ is refined at both 280 and 3.5 K from neutron powder data, and magnetic properties are reported for the first time. The scheelite structure, $I4_1/a$, is confirmed at both temperatures. Atomic positions of greater accuracy than the original 1954 X-ray study are reported. The rare Ru⁷⁺ ion resides in a site of distorted tetrahedral symmetry with nominal electronic configuration 4d¹(e¹). Curie–Weiss parameters are near free ion values for the effective moment and $\theta = -77$ K, indicating dominant antiferromagnetic (AF) correlations. A broad susceptibility maximum occurs near 34 K, but long-range AF order sets in only below 22.4 K as determined by magnetization and heat capacity data. The entropy loss below 50 K is only 44% of the expected $R \ln 2$, indicating the presence of short-range spin correlations over a wide temperature range. The Ru sublattice consists of centered, corner-sharing tetrahedra which can lead to geometric frustration if both the nearest-neighbor, J_1 , and the next-nearest-neighbor, J_2 , exchange constants are AF and of similar magnitude. A spin dimer analysis finds $J_1/J_2 \approx 25$, indicating weak frustration, and a (d_z²)¹ ground state. A single, weak magnetic reflection was indexed as (110). The absence of the (002) magnetic reflection places the Ru moments parallel to the *c* axis. The Ru⁷⁺ moment is estimated to be 0.57(7) μ_B , reduced from an expected value near 1 μ_B . A recent computational study of isostructural, isoelectronic KOsO₄ predicts a surprisingly large orbital moment due to spin–orbit coupling (SOC). However, the free ion SOC constant for Ru⁷⁺ is only $\sim 30\%$ that of Os⁷⁺, so it is unclear that this effect can be implicated in the low ordered moment for KRuO₄. The origin of the short-range spin correlations is also not understood.



INTRODUCTION

KRuO₄, potassium perruthenate, is a well-known reagent for oxidation of primary alcohols to carbonyls.¹ It crystallizes in the scheelite structure, $I4_1/a$, as reported more than 60 years ago.² In that study the Bragg intensities were measured from films, and the accuracy of the structural details is not to modern standards. KRuO₄ involves the rare Ru⁷⁺ ion which has electronic configuration 4d¹, and as the Ru site is a distorted tetrahedron, it is nominally e¹. There have been no reports of the magnetic properties of this material. The Ru sublattice consists of an array of centered, corner-sharing tetrahedra, Figure 1, and thus, the possibility of geometrically frustrated magnetism is present, particularly if the nearest-neighbor, J_1 , and next-nearest-neighbor, J_2 , exchange constants are antiferromagnetic and of similar magnitude. In this study the structure of KRuO₄ was refined from powder neutron diffraction data both at ambient temperature and at 3.5 K. The magnetic susceptibility and heat capacity were measured

and reported for the first time. The magnetic properties suggest some level of either short-range spin correlations or geometric frustration which occur above the observed Néel temperature of 22.4 K. The exchange constants J_1 and J_2 were estimated using spin dimer analysis.³

EXPERIMENTAL DETAILS

KRuO₄ is a commercially available oxidizing agent and was purchased from Alfa Aesar (99% claimed purity) and used without further purification.

Neutron Powder Diffraction. Neutron powder diffraction data were obtained at the Canadian Neutron Beam Centre, at the Canadian Nuclear Laboratories, Chalk River, Ontario, Canada. The C2 diffractometer was used with neutron wavelengths of 1.33 and 2.37 Å. The wavelengths were calibrated against a standard Al₂O₃ sample. The sample was contained in both thin-walled vanadium and

Received: September 20, 2016

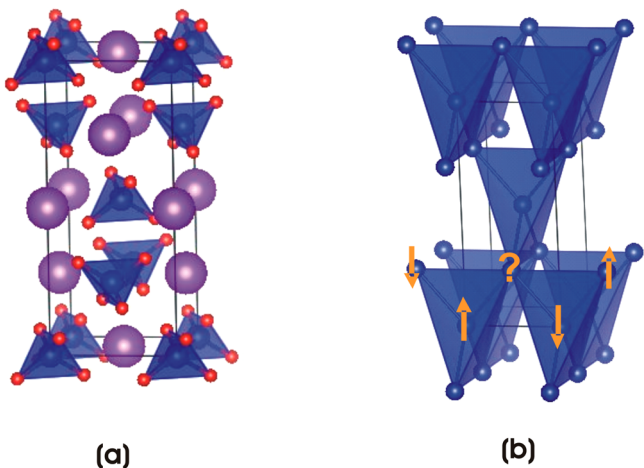


Figure 1. (a) Unit cell of KRuO_4 . Ru ions are blue, oxide ions are red, and K ions are violet. (b) Ru sublattice consisting of an array of centered, corner-sharing tetrahedra. Arrows indicate the situation in which J_1 (connecting the centered ion to the corners of the tetrahedron) and J_2 (connecting ions on the corners of the tetrahedron) are both AF and of similar magnitude which leads to geometric frustration.

aluminum cans and placed in a closed cycle cryostat. Data were obtained both at ambient temperature, 280 K, and at base temperature, 3.5 K.

Magnetic Properties. Magnetization data were obtained with a Quantum Design M.P.M.S. SQUID magnetometer over the temperature range from 320 to 2 K.

Heat Capacity. Heat capacity measurements were performed using pellets of 4–8 mg, weighed to an accuracy of $\pm 2 \mu\text{g}$, placed on an 8-wire sapphire platform sample stage of a Dynacool Physical Property Measurement System (Quantum Design). The pellets were adhered to the platform using Apiezon N-grease during the measurements which were performed in a zero magnetic field over the temperature range from 2 to 100 K. The heat capacity of the puck and grease were subtracted from the total heat capacity.

■ RESULTS AND DISCUSSION

Crystal Structure. The refinement of the neutron powder diffraction data taken at 280 and 3.5 K is shown in Figure 2, and the results are displayed in Table 1. The scheelite structure is described in $I4_1/a$. The first origin choice was taken with Ru in 4a (0 1/4 1/8), K in 4b (0 1/4 5/8), and O in 16f (x, y, z). Note that the refined Ru–O distance, 1.742(4) Å, agrees very well with the sum of the ionic radii $\Sigma[r(\text{Ru}^{7+}) + r(\text{O}^{2-})] = 1.74$ Å, where the IV-fold radius is taken for Ru^{7+} and the III-fold radius for O^{2-} .⁴ The interatomic distances are of course more precise and accurate than those of the original study, as this was based on Weissenberg film data.² Some of the residuals, especially χ^2

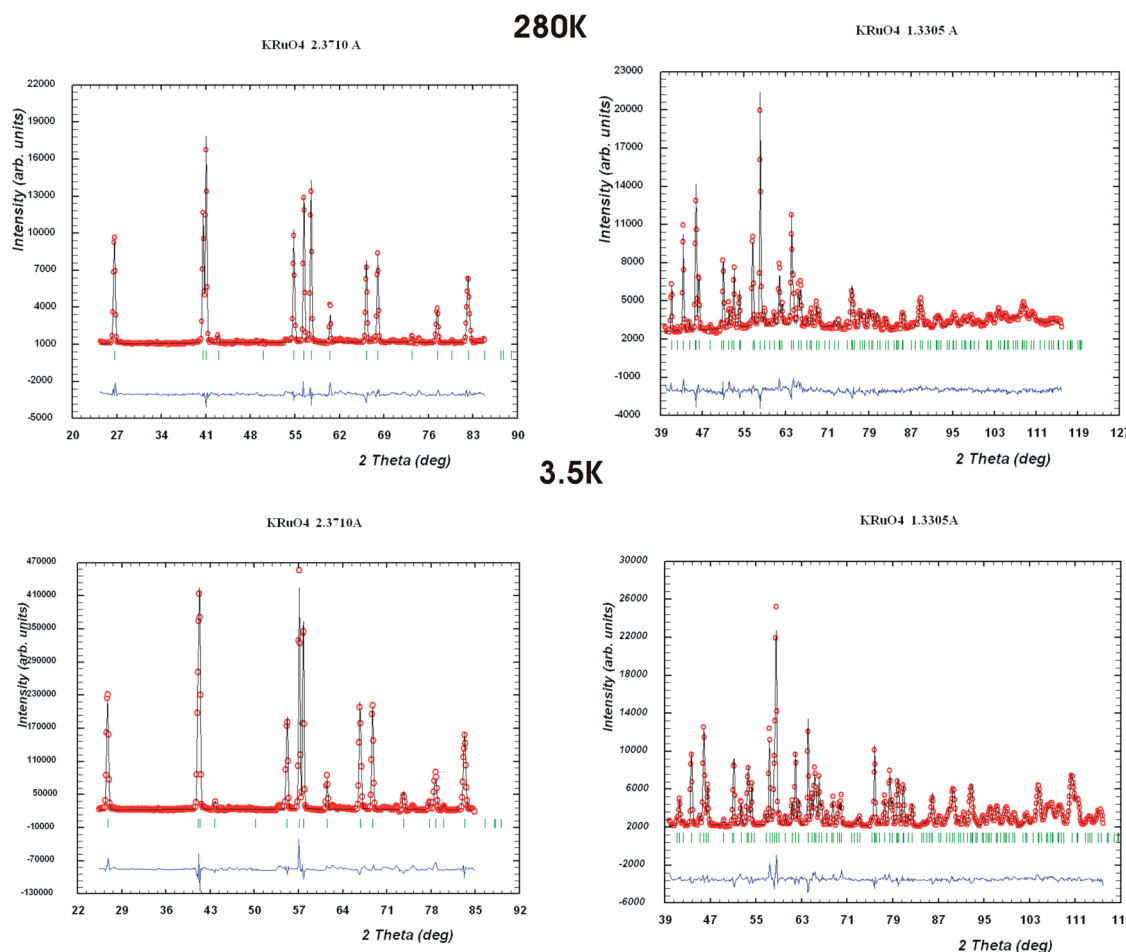


Figure 2. Results of a Rietveld refinement of neutron powder diffraction data for KRuO_4 at 280 (top) and 3.5 K (bottom). For the left-hand panel $\lambda = 2.3710$ Å, and for the right-hand panel $\lambda = 1.3305$ Å. Red circles are the data, black line is the calculated pattern, blue line is the difference, and green vertical tic marks locate the Bragg peaks.

Table 1. Refinement Results for KRuO_4 ^a

	3.5 K	280 K
<i>a</i> (Å)	5.6048(3)	5.6105(5)
<i>c</i> (Å)	12.7597(7)	12.959(1)
Ox	0.1177(4)	0.1113(6)
Oy	0.0193(4)	0.0162(8)
Oz	0.1999(2)	0.1992(3)
<i>B</i> (K) (Å ²)	0.05(7)	1.54(14)
<i>B</i> (Ru) (Å ²)	0.20(5)	1.61(11)
<i>B</i> (O) (Å ²)	0.49(4)	2.57(9)
<i>V</i> (Å ³)	400.8	407.9
Ru–O (Å)	1.738(2)	1.742(4)
K–O (Å)	2.790(2)	2.813(4)
	2.776(2)	2.795(4)
O–Ru–O (deg)	107.6(2)	107.7(3)
	113.3(2)	113.0(4)
<i>R</i> _{wp} , χ^2	5.58, 11.1	4.70, 6.649
<i>R</i> _F	4.40	9.51

^aThe first origin choice for $I4_1/a$ was taken with Ru in 4a (0 1/4 1/8), K in 4b (0 1/4 5/8), and O in 16f (*x,y,z*).

at 3.5 K, are larger than expected. This is due to the presence of an unidentified second phase which could not be fully excluded from the refinement. Note that R_F , which is somewhat independent of the profile fit, is acceptable, especially at 3.5 K.

Magnetic Properties. The magnetic data are summarized in Figure 3. Note the broad maximum near 35 K and a pronounced ZFC/FC divergence near 22 K, Figure 3a. The

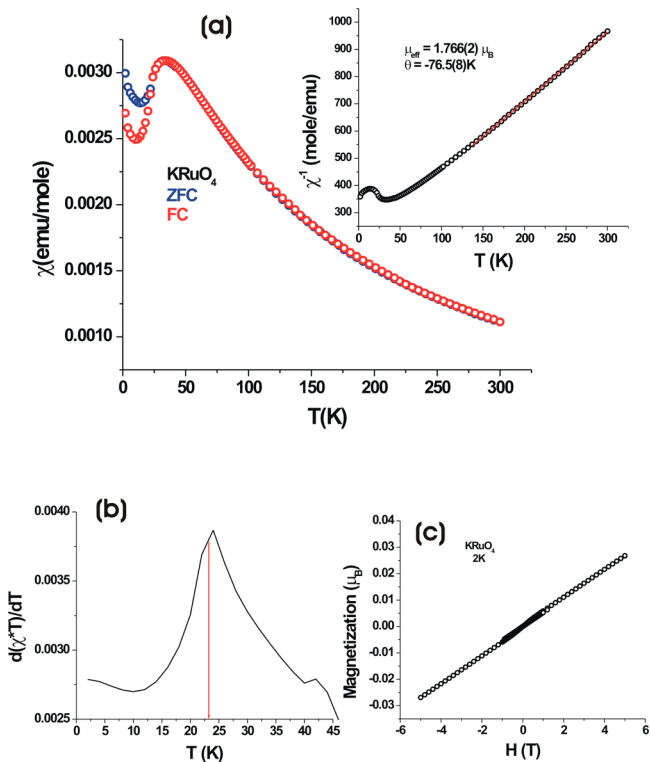


Figure 3. (a) Magnetic susceptibility of KRuO_4 . Note the broad maximum at ~ 35 K and the ZFC/FC divergence near 22 K. (b) Fisher heat capacity, $d(\chi^*)/dT$ vs T , locating the true Néel temperature at ~ 22.5 K. (c) Linear dependence of the magnetization with applied field at 2 K, consistent with AF order.

Curie-Weiss law, see inset, is obeyed above about 150 K, yielding an effective moment near the free ion value of $1.73 \mu_B$ and $\theta = -76.5(8) \text{ K}$, indicative of antiferromagnetic (AF) spin correlations. The true Néel temperature, Figure 3b, is located by plotting the Fisher heat capacity, $d(\chi^*)/dT$ vs T , and is seen to be near 22.5 K.⁵ The magnetization at 2 K, Figure 3c, is linear, consistent with the AF order.

Heat Capacity. The heat capacity for KRuO_4 in zero applied magnetic field is shown in Figure 4a along with a proposed lattice match material, isostructural KReO_4 . A clear lambda anomaly appears at 22.4(1) K, consistent with the magnetization studies, Figure 4b. The heat capacity remains essentially unchanged upon application of a 9 T magnetic field (SI Figure 1). Taken together, the magnetization and heat capacity data provide convincing evidence for long-range AF order in this material below 22.4 K. While the heat capacity of the lattice match material is not ideal, it appears to be slightly too large at low temperatures and slightly too small at high temperatures; nonetheless, a direct subtraction was done with the results shown in Figure 4c. Note the negative values from 2 to 14 K. The entropy loss, S , computed with $T_{\text{max}} = 50$ K and $T_{\text{min}} = 14$ K, Figure 4d, is 2.26 eu, only 44% of $R \ln 2 = 5.76$ eu. ΔS associated with the lambda anomaly, $T_{\text{max}} = 25$ K, is only 1.21 eu (21% of $R \ln 2$). These observations are consistent with significant short-range spin correlations for KRuO_4 , due either to frustration effects or to low dimensionality.

Magnetic Neutron Diffraction. In an attempt to determine the magnetic structure and to measure the ordered moment at the Ru⁷⁺ site, neutron diffraction data were collected at 3.5 K, well below T_N . Careful examination of data at 280 and 3.5 K showed the presence of a single, very weak magnetic reflection which can be indexed as (110), indicating that $\mathbf{k} = (000)$, Figure 5. Note that (110) is systematically absent in $I4_1/a$. The presence of this reflection and the absence of a magnetic (002) reflection indicates that the Ru moments are parallel to the *c* axis. Reflections of the type (00*l*), $l \neq 4n$, are also systematically absent; however, simulations of the magnetic diffraction pattern with the Ru moment in the *ab* plane show significant intensity at (002) as would be expected.

This analysis points to the model of Figure 6 for which $J_1 < 0$ and $|J_1| \gg |J_2|$, where J_1 and J_2 are the nearest-neighbor and next-nearest-neighbor exchange constants, respectively. In terms of representation analysis, of the four irreducible representations of $I4_1/a$ with $\mathbf{k} = (000)$, which are $\Gamma_1, \Gamma_3, \Gamma_5$, and Γ_7 , only Γ_5 yields a basis vector consistent with the data, i.e., an AF structure with moments along the *c* axis.

An attempt was made to refine the Ru moment on this model, but given the very weak intensity of the lone magnetic peak, the ratio $I(110)_{\text{MAG}}/I(101)_{\text{NUCL}}$ is only 0.86%, unreasonably small values, near $0.2 \mu_B$, with extremely large errors, ($\pm 0.5 \mu_B$), resulted. Thus, another approach was taken to estimate the ordered Ru moment. Diffraction patterns with a magnetic component based on the model in Figure 6 were simulated with various moments on the Ru site, and the expected $I(110)/I(\text{NUCL})$ ratio was determined as a function of the Ru moment for two nuclear reflections, (101) and (004). The former has a small magnetic contribution of the order 2%. As shown in Figure 7 the experimental intensity ratios are $I(110)/I(101) = 0.0086(9)$ and $I(110)/I(004) = 0.20(3)$. In the simulations, as there is no published magnetic form factor for Ru⁷⁺, $f(Q)$ for both Ru¹⁺ and Os⁵⁺ were used.^{6,7} The differences in calculated intensity ratios were within the experimental error. These results are shown in Figure 7, and the estimated Ru⁷⁺

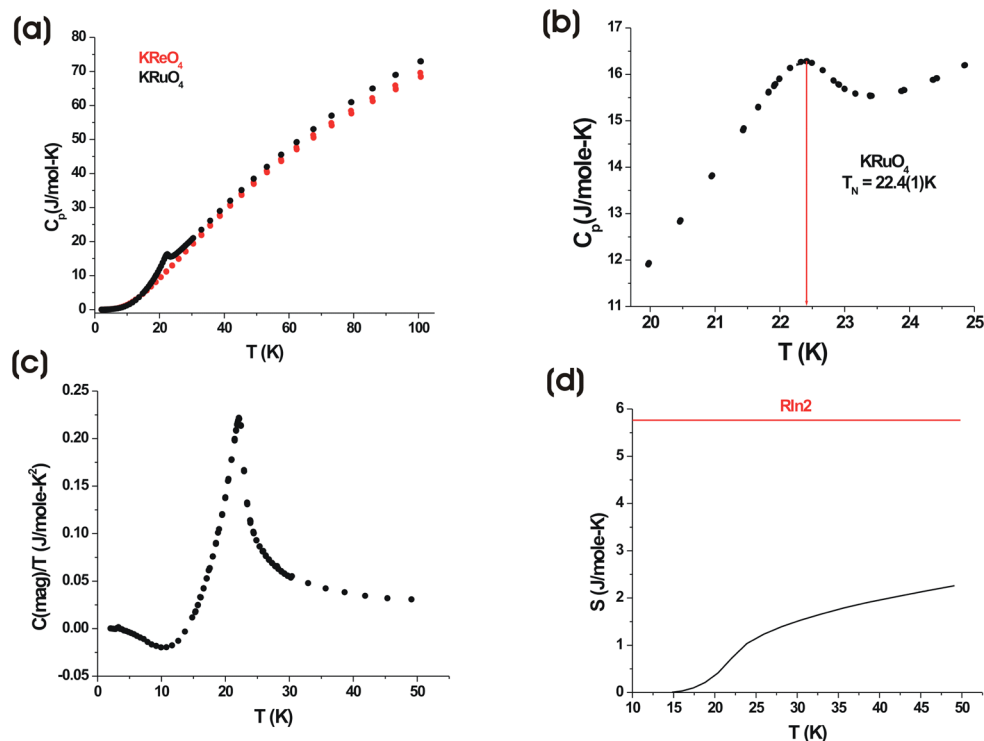


Figure 4. (a) Heat capacity of KRuO₄ in zero applied magnetic field compared with that for the lattice match material, isostructural KReO₄. (b) Maximum at $T_N = 22.4(1)$ K. (c) $C(\text{mag})/T$ versus T obtained by direct subtraction of the heat capacity of KReO₄. Note the negative values from 4 to 14 K. (d) Entropy loss (S) over the range 50–14 K compared with $R \ln 2$.

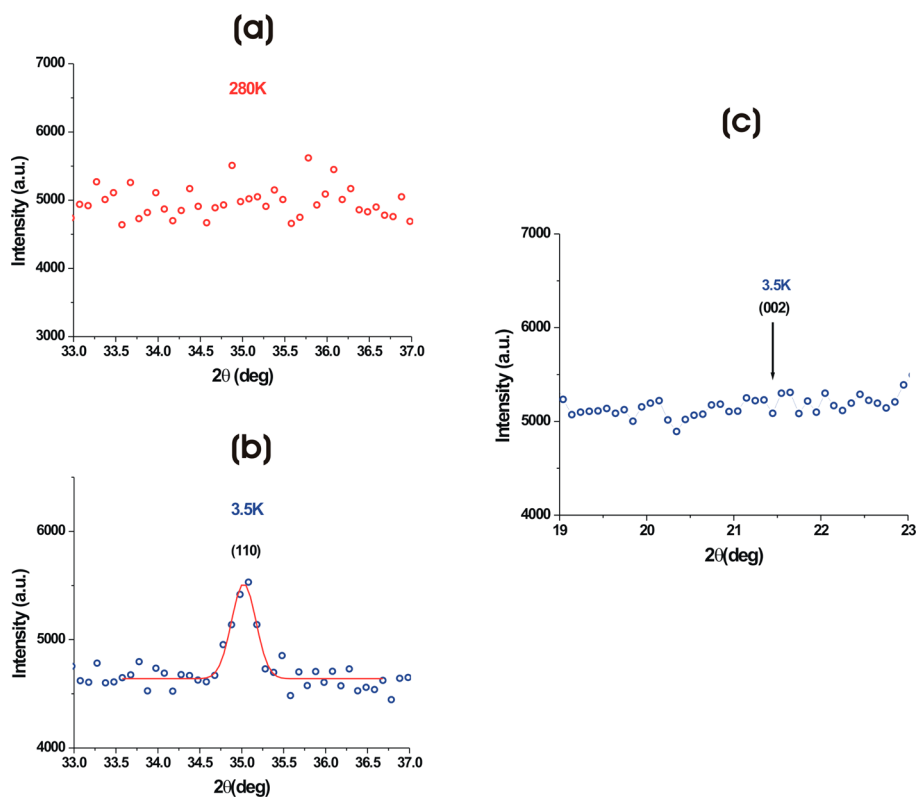


Figure 5. Comparison of neutron diffraction data at 280 (a) and 3.5 K (b and c) for KRuO₄. Note the presence of a very weak Bragg peak at 35° and 3.5 K which can be indexed as (110), i.e., $k = (000)$. (The fit is to a single Gaussian with a resolution-limited peak width.) (c) Absence of the (002) reflection which indicates that the Ru moment is parallel to the c axis.

ordered moment is $0.57(7) \mu_B$, taking an average for the two analyses.

Thus, the ordered moment is reduced significantly from the free ion value of $\sim 1 \mu_B/\text{Ru}^{7+}$ ion, by $\sim 40\%$. Such a low

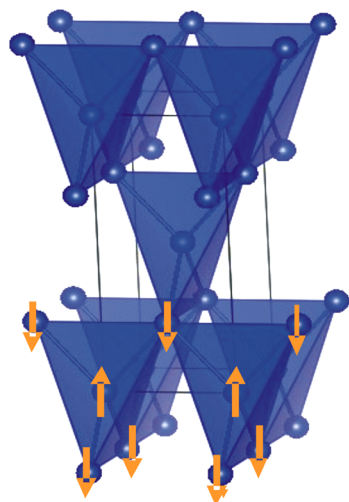


Figure 6. $k = (000)$ magnetic structure consistent with the magnetic neutron diffraction data. For clarity, not all spins are shown.

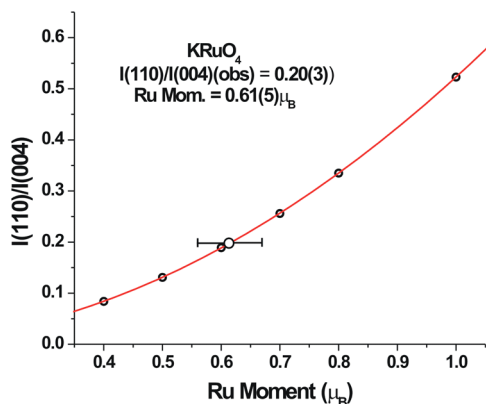
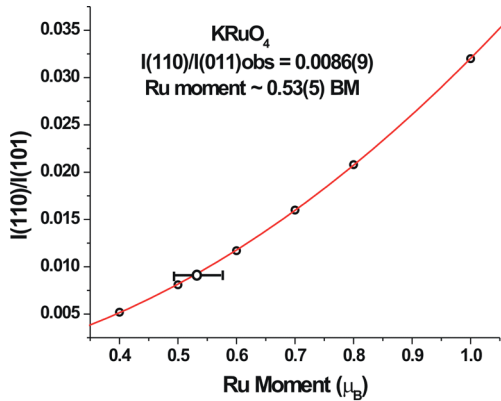


Figure 7. Estimate of the Ru ordered moment in KRuO₄ by comparison of observed and calculated $I(110)/I(101)$ and $I(110)/I(004)$ ratios. Ru moment is $0.57(5) \mu_B$.

moment is somewhat difficult to reconcile with existing literature. For example, studies of the RuO₄⁻ ion in solution via electron spin resonance report g factors near 2.⁸ Also, the $(d_z^2)^1$ state is an orbital singlet and spin-orbit coupling is expected to be weak. However, a recent computational study of isostructural and isoelectronic KOsO₄ indicates that spin-orbit coupling (SOC) can be surprisingly strong in distorted e^1 systems, contrary to common wisdom, in spite of the fact that SOC is a higher order effect in orbital singlets.⁹ Orbital singlet

ground states result of course from the tetrahedral distortions.¹⁰ However, the SOC constant for a 4d ion is usually about 20–30% of that for the corresponding 5d ion,¹¹ so it is unclear without further study whether SOC can explain the smallish ordered Ru⁷⁺ moment in KRuO₄.

Geometric Frustration or Low-Dimensional Magnetism? Finally, the susceptibility data of Figure 3, which show a broad maximum at ~ 35 K, well above the true T_N of 22.5 K, indicate the presence of either frustrated or low-dimensional magnetism in KRuO₄. The frustration index, $f = |\theta|/T_N = 3.4$, does not support a strong argument for geometric magnetic frustration.¹² As pointed out in Figure 1, geometric frustration would be favored for the case $J_1 \approx J_2$ and both AF. To investigate this further, spin dimer calculations using CAESAR were undertaken.³ The results are shown in Figure 8 and Table

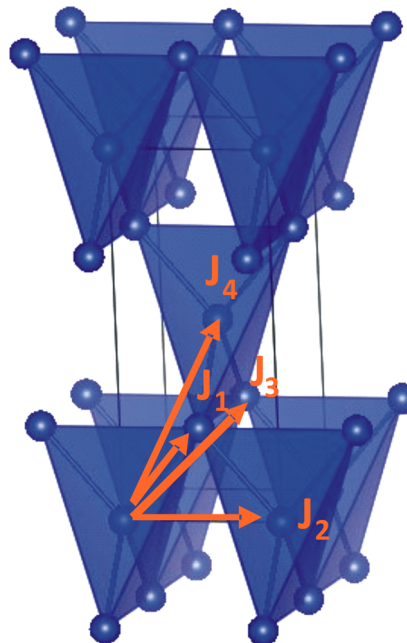


Figure 8. Exchange pathways for which a spin dimer calculation was done. J_1 and J_2 are the nearest-neighbor and next-nearest-neighbor interactions, respectively.

Table 2. Results of the Spin Dimer Calculation for the Various J_n Identified in Figure 8

n	$J(\text{rel})$
1	1.0
2	0.043
3	3.5×10^{-5}
4	1.86×10^{-5}

2. The details are given in the SI. In these calculations it is clear that the e^1 state is split by the distortion of the tetrahedron and that the d_z^2 orbital is the ground state, consistent with the proposed magnetic structure. As can be seen from Table 2, the J_1 pathway is dominant and the J_1/J_2 ratio is ~ 25 . From these results the actual sign of J_2 is ambiguous, as, in the spin dimer method, small values of J can indicate the interaction of orthogonal orbitals, which implies ferromagnetism. The results of Table 2 are further evidence against an argument for strong geometric frustration.

A second possibility to explain the discrepancy between $T(\chi_{\text{MAX}})$ and T_{N} , $T(\chi_{\text{MAX}})/T_{\text{N}} = 1.5$, involves low-dimensional spin correlations. While it is also not clear that low dimensionality is supported by the results of Table 2, fits to both $S = 1/2$ one-dimensional and two-dimensional spatial models were undertaken. The Heisenberg model was taken for the spin dimensionality. While both gave fits of similar quality, the one-dimensional fit required a g factor > 3 , which is impossible. The fit to the two spatial dimensional model is shown in Figure 9. The fitting function used is for a $S = 1/2$

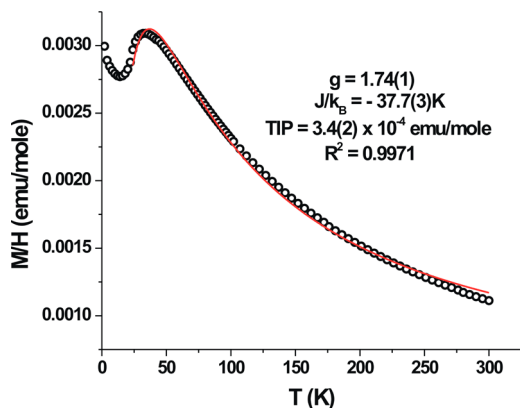


Figure 9. Fit to the susceptibility data for KRuO₄ using a model for $S = 1/2$ Heisenberg spins on a square lattice.

square lattice Heisenberg model.¹³ There are only three parameters, g , J/k_B , and a temperature-independent susceptibility (TIP). The fit gives a reasonable g factor 1.74(1) and $J/k_B = -37.7(3)$ K. The TIP seems large. While the fit to the two-dimensional square lattice model is not unreasonable, it cannot be taken as definitive evidence for a low-dimensional model. Further computational work is clearly needed.

SUMMARY AND CONCLUSIONS

The crystal structure of the common organic oxidizing agent, KRuO₄, has been refined from neutron powder diffraction data at both ambient temperature and 3.5 K, confirming the scheelite structure and improving on the original X-ray film study. The magnetic properties are reported for the first time and present some interesting problems. In this material the rare Ru⁷⁺ ion resides in a distorted tetrahedral site with nominal electronic configuration e^1 . Magnetization and heat capacity studies show unequivocal evidence for long-range AF order below $T_{\text{N}} = 22.4(1)$ K, while the magnetic susceptibility shows a broad maximum at 34 K. The entropy loss below 50 K is only 44% of the expected $R \ln 2$, indicating the presence of short-range spin correlations over a wide temperature range, consistent with the magnetization data. A single very weak magnetic neutron diffraction peak was observed and indexed as (110). A (002) reflection was not observed, indicating that the Ru moments are along the c axis, consistent with a d_z^2 ground state. The ordering wave vector is $k = (000)$, and a magnetic structure is proposed with an ordered moment on Ru⁷⁺ of 0.57(7) μ_{B} . This is not easy to reconcile with either the susceptibility or e.s.r. data on the RuO₄⁻ ion in solution, both of which suggest a g factor near the free ion value of 2 and thus an ordered moment near 1 μ_{B} . Also, moment reduction via SOC for orbital singlets is expected to be weak. While the case of isostructural KOsO₄ may be a guide to understanding the

puzzling features of the ruthenium analog, SOC for 4d ions is typically only 20–30% that for 5d ions. The origin of the short-range spin correlations well above T_{N} was addressed. Arguments for the role of geometric frustration were deemed to be weak due to a small frustration index of ~ 3 and a spin dimer computational analysis which indicated that the conditions for frustration are not present. The possibility of short-range, low-dimensional spin correlations was also considered and a $S = 1/2$ Heisenberg model on a square lattice cannot be ruled out. Much further work is needed, both computational, at a higher level than the spin dimer model, and experimentally on single crystals to better measure the Ru⁷⁺ moment and perhaps to observe diffuse magnetic scattering which might afford some insight into the origins of the short-range spin correlations.

ASSOCIATED CONTENT

Supporting Information

The Supporting Information is available free of charge on the ACS Publications website at DOI: [10.1021/acs.inorgchem.6b02284](https://doi.org/10.1021/acs.inorgchem.6b02284).

Heat capacity of KRuO₄ at an applied field of 9 T, details of the CAESAR calculations ([PDF](#))
CIFs at 3.5 and 280 K ([PDF](#))

AUTHOR INFORMATION

Corresponding Author

*E-mail: greedan@mcmaster.ca.

ORCID 

John E. Greedan: [0000-0003-1307-8379](https://orcid.org/0000-0003-1307-8379)

Notes

The authors declare no competing financial interest.

ACKNOWLEDGMENTS

J.E.G., B.D.G., and C.R.W. thank the Natural Sciences and Engineering Research Council of Canada for support through a Discovery Grant. C.R.W. also acknowledges support from the Canadian Foundation for Innovation and the Canada Research Chair program, Tier II. P. Dube assisted with collection of magnetization data.

REFERENCES

- Wu, D. L.; Wight, A. P.; Davis, M. E. Shape selective oxidation of primary alcohols using perruthenate-containing zeolites. *Chem. Commun.* 2003, 758–759.
- Silverman, M. D.; Levy, H. A. Crystal Structure of potassium perruthenate, KRuO₄. *J. Am. Chem. Soc.* 1954, 76, 3317–3319.
- Whangbo, W. H.; Koo, H. J.; Dai, D. Spin exchange interactions and magnetic structures of magnetic extended solids with localized spins: theoretical descriptions on formal, quantitative and qualitative levels. *J. Solid State Chem.* 2003, 176, 417–481. Ren, J.; Liang, W.; Whangbo, M. H. *Crystal and Electronic Structure Analysis Using CAESAR*; 2005; <http://www.primeC.com>.
- Shannon, R. D. Revised Effective Ionic Radii and Systematic Studies of Interatomic Distances in Halides and Chalcogenides. *Acta Crystallogr., Sect. A: Cryst. Phys., Diffr., Theor. Gen. Crystallogr.* 1976, 32, 751–767.
- Fisher, M. E. Relation between the specific heat and susceptibility of an antiferromagnet. *Philos. Mag.* 1962, 7, 1731–1743.
- Brown, P. J. Magnetic Form Factors. *International Tables of Crystallography*; Kluwer Academic Publishers, Dordrecht, 1992; Vol. C, p 393.

(7) Kobayashi, K.; Nagao, T.; Ito, M. Radial integrals for the magnetic form factor for 5d transition elements. *Acta Crystallogr., Sect. A: Found. Crystallogr.* **2011**, *67*, 473–480.

(8) Dengel, A. C.; Gibson, J. F.; Griffith, W. P. Electron Spin Resonance Spectra of the Perruthenate(VII) Ion, RuO_4^- . *J. Chem. Soc., Dalton Trans.* **1991**, 2799–2800.

(9) Song, Y.-J.; Ahn, K.-H.; Lee, K.-W.; Pickett, W. E. Unquenched e_g^1 orbital moment in the Mott-insulating antiferromagnet KO_4OsO_4 . *Phys. Rev. B: Condens. Matter Mater. Phys.* **2014**, *90*, 245117.

(10) Di Gregorio, S.; Greenblatt, M.; Pifer, J. H.; Sturge, M. D. An ESR and optical study of V^{4+} in zircon-type crystals. *J. Chem. Phys.* **1982**, *76*, 2931–2937.

(11) Ma, C.-G.; Brik, M. G. Systematic analysis of spectroscopic characteristics of heavy transition metal ions with 4d^N and 5d^N ($N = 1\text{--}10$) configurations in a free state. *J. Lumin.* **2014**, *145*, 402–409.

(12) Ramirez, A. P. Strongly Geometrically Frustrated Magnets. *Annu. Rev. Mater. Sci.* **1994**, *24*, 453–480.

(13) Rushbrooke, G.; Wood, P. J. On the high temperature staggered susceptibility of Heisenberg antiferromagnets. *Mol. Phys.* **1963**, *6*, 409–421.